Coexistence of Ferromagnetic and Stripe Antiferromagnetic Spin Fluctuations in SrCo$_2$As$_2$

Yu Li,[1,2] Zhiping Yin,[2,*] Zhonghao Liu,[3,†] Weiyi Wang,[1] Zhuang Xu,[2] Yu Song,[1] Long Tian,[2] Yaobo Huang,[4]
Dawei Shen,[3] D. L. Abernathy,[5] J. L. Niedziela,[5] R. A. Ewings,[6] T. G. Perring,[6] Daniel M. Pajerowski,[5]
Masaaki Matsuda,[5] Philippe Bourges,[7] Enderle Mechthild,[8] Yixi Su,[9] and Pengcheng Dai[1,2,‡]

[1]*Department of Physics and Astronomy, Rice University, Houston, Texas 77005, USA*
[2]*Department of Physics, Beijing Normal University, Beijing 100875, China*
[3]*State Key Laboratory of Functional Materials for Informatics and Center for Excellence in Superconducting Electronics, SIMIT,
Chinese Academy of Sciences, Shanghai 200050, China*
[4]*Shanghai Synchrotron Radiation Facility, Shanghai Institute of Applied Physics, Chinese Academy of Sciences,
Shanghai 201204, China*
[5]*Neutron Scattering Division, Oak Ridge National Laboratory, Oak Ridge, Tennessee 37831, USA*
[6]*ISIS Pulsed Neutron and Muon Source, STFC Rutherford Appleton Laboratory, Didcot, Oxfordshire, OX11 0QX, United Kingdom*
[7]*Laboratoire Léon Brillouin, CEA-CNRS, Université Paris-Saclay, CEA Saclay, 91191 Gif-sur-Yvette, France*
[8]*Institut Laue-Langevin, 6 rue Jules Horowitz, Boîte Postale 156, 38042 Grenoble Cedex 9, France*
[9]*Jülich Centre for Neutron Science (JCNS) at Heinz Maier-Leibnitz Zentrum (MLZ),
Forschungszentrum Jülich, Lichtenbergstrasse 1, 85747 Garching, Germany*

We use inelastic neutron scattering to study energy and wave vector dependence of spin fluctuations in SrCo$_2$As$_2$, derived from SrFe$_{2-x}$Co$_x$As$_2$ iron pnictide superconductors. Our data reveal the coexistence of antiferromagnetic (AF) and ferromagnetic (FM) spin fluctuations at wave vectors $\mathbf{Q}_{AF} = (1,0)$ and $\mathbf{Q}_{FM} = (0,0)/(2,0)$, respectively. By comparing neutron scattering results with those of dynamic mean field theory calculation and angle-resolved photoemission spectroscopy experiments, we conclude that both AF and FM spin fluctuations in SrCo$_2$As$_2$ are closely associated with a flatband of the e_g orbitals near the Fermi level, different from the t_{2g} orbitals in superconducting SrFe$_{2-x}$Co$_x$As$_2$. Therefore, Co substitution in SrFe$_{2-x}$Co$_x$As$_2$ induces a t_{2g} to e_g orbital switching, and is responsible for FM spin fluctuations detrimental to the singlet pairing superconductivity.

Flat electronic bands can give rise to a plethora of interaction-driven quantum phases, including ferromagnetism [1], a Mott insulating phase due to electron correlations [2], and superconductivity [3]. Therefore, an understanding of how the flat electronic bands can influence the electronic, magnetic, and superconducting properties of solids is an important topic in condensed matter physics. In iron pnictide superconductors such as AFe$_{2-x}$Co$_x$As$_2$ (A = Ba, Sr) [Figs. 1(a)–1(d)], the dominant interactions are stripe antiferromagnetic (AF) order, and superconductivity, which has singlet electron pairing, arises by doping an electron with Co substitution to suppress static AF order [4–6]. While AF spin fluctuations and superconductivity in iron pnictides are believed to arise from nested hole Fermi surfaces at Γ and electron Fermi surfaces at M [Fig. 1(e)] [7], the density functional theory (DFT) calculations suggest competing ferromagnetic (FM) and AF spin fluctuations with the balance controlled by doping [8,9]. For Co-overdoped ACo$_2$As$_2$ [10,11], where the DFT calculations find a tendency for both the FM and AF order, neutron scattering revealed only the AF spin fluctuations [12] while angle-resolved photoemission spectroscopy (ARPES) experiments found no evidence of the Fermi surface nesting [13,14]. On the other hand, nuclear magnetic resonance (NMR) measurements on AFe$_{2-x}$Co$_x$As$_2$ provided evidence for FM spin fluctuations at all Co-doping levels in addition to the AF spin fluctuations [15,16]. In particular, strong FM spin fluctuations in AFe$_{2-x}$Co$_x$As$_2$ are believed to compete with AF spin fluctuations and prevent superconductivity for Co-overdoped samples [15,16], contrary to the Fermi surface nesting picture where superconductivity is suppressed via vanishing hole Fermi surfaces with increasing Co doping [7,17]. Finally, action of physical, chemical pressure, or aliovalent substitution in BCo$_2$As$_2$ (B = Eu, Ca) can drive these AF materials into ferromagnets [18]. In particular, CaCo$_{1.84}$As$_2$ with a collapsed tetragonal structure [19] forms an A-type AF ground state with coexisting FM spin fluctuations within the CoAs layer and A-type AF spin fluctuations between the CoAs layers [20]. These features are different from those of Ca(Fe$_{1-x}$Co$_x$)$_2$As$_2$ [21,22] and AFe$_{2-x}$Co$_x$As$_2$ [6].
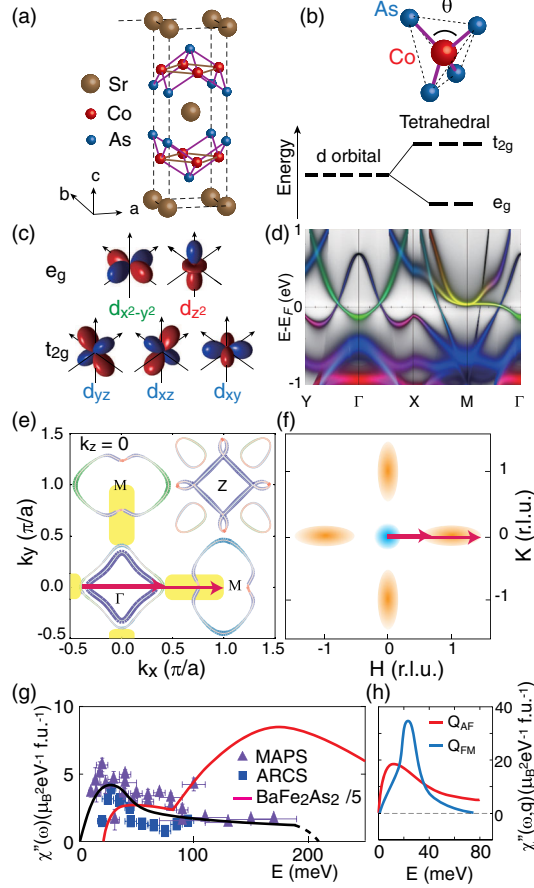
FIG. 1. (a) Crystal structure of $SrCo_2As_2$. (b) The tetrahedron of $Fe(Co)As_4$ and the resulting d-orbital splitting. (c) Wave functions of the five d orbitals. (d) Band structure of $SrCo_2As_2$. Green (red) represents the $d_{x^2-y^2}$(d_{z^2}) orbital and blue is the contribution from the t_{2g} (d_{xz}, d_{yz}, d_{xy}) orbitals. Yellow is the mixture of red (d_{z^2}) and green ($d_{x^2-y^2}$). (e) Fermi surfaces from DFT + DMFT calculations. The shading yellow area corresponds to the flatband (yellow part) in Fig. 1(d) and arrows represent scattering wave vectors associated with the flatband. The colors represent the same orbital characters as in (c) and (d). (f) Schematics of the low energy FM (blue) and AF (orange) spin fluctuations in $SrCo_2As_2$. (g) Energy dependence of integrated $\chi''(E)$ of $SrCo_2As_2$ in absolute units normalized by using a vanadium standard [23]. The red solid line is $\chi''(E)/5$ of $BaFe_2As_2$ [28]. The black solid line is a guide to the eye. (h) The measured AF and FM fluctuations at Q_{AF} and Q_{FM} [23].

Iron pnictides have five nearly degenerate d orbitals which split into t_{2g} and e_g orbitals in a tetrahedral crystal field [Figs. 1(b) and 1(c)]. The electronic structure of the system is dominated by Fe $3d$ t_{2g} orbitals near the Fermi level with hole-electron Fermi surfaces at Γ and M, respectively [Fig. 1(e)]. The presence of multiple Fe $3d$ orbitals near the Fermi level results in varying orbital characters on different parts of the Fermi surfaces [29], and orbital-dependent strengths of electronic correlations [30–34]. The electronic band structures of $SrCo_2As_2$ calculated by DFT combined with dynamic mean field
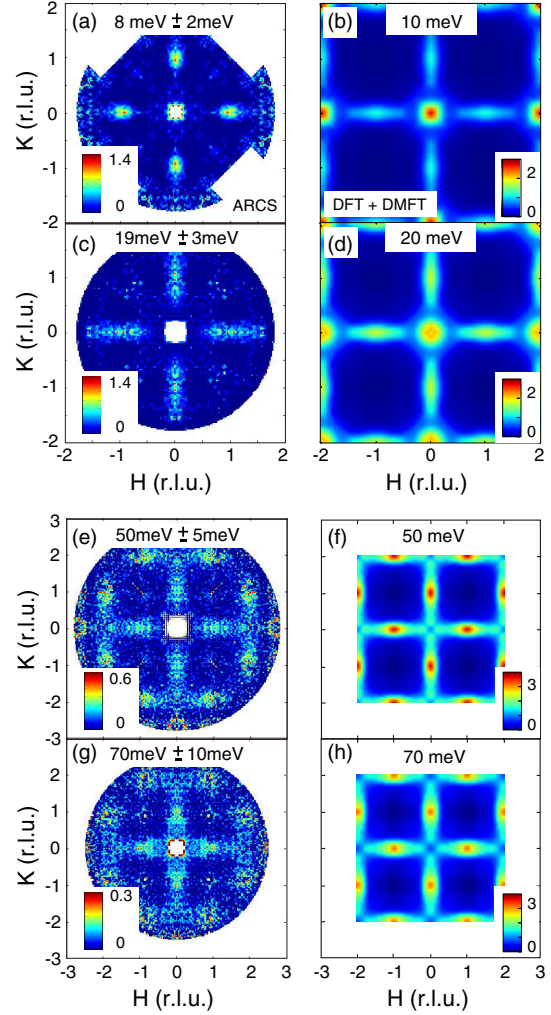

FIG. 2. (a),(c),(e),(g) Two-dimensional images of measured dynamic spin susceptibility of $SrCo_2As_2$ in the $[H, K]$ plane at $E = 8 \pm 2$, 19 ± 3, 50 ± 5, and 70 ± 10 meV, respectively. Radially symmetric backgrounds were subtracted to visually enhance the weak magnetic signal. (b),(d),(f),(h) The corresponding results from the DFT + DMFT calculations [23].

theory (DMFT) [35,36] reveal the presence of a flatband near the M point with a mixture of the d_{z^2} and $d_{x^2-y^2}$ orbitals [Fig. 1(d)]. If $SrCo_2As_2$ has a strong ferromagnetism arising from the flatband as suggested from NMR [15,16], one should be able to extract its energy and wave vector dependence by neutron scattering and determine its role to the suppressed superconductivity in Co-overdoped $SrFe_{2-x}Co_xAs_2$ [4–6].

In this Letter, we combine neutron scattering, ARPES, and DFT + DMFT methods to study $SrCo_2As_2$, an electron-doped end member of $SrFe_{2-x}Co_xAs_2$ exhibiting no structural, magnetic, or superconducting transitions [11]. Besides confirming the longitudinally elongated AF spin fluctuations at wave vector $Q_{AF} = (1, 0)$ [Figs. 1(f) and 2] [12], we successfully observed the in-plane FM spin fluctuations at $Q_{FM} = (0, 0)$ and its equivalent $(2, 0)$

positions [Figs. 2 and 3]. From the DFT + DMFT calculations and ARPES measurements, we find a flatband consisting of the e_g orbitals along the Γ-M direction right above the Fermi level [Fig. 1(d)], leading to a prominent peak in the density-of-state (DOS) near Fermi level responsible for both the FM and AF spin fluctuations [Figs. 4(a)–4(d)]. Orbital analysis of the dynamic spin susceptibility $\chi''(\mathbf{Q}, E)$ in the DFT + DMFT calculations suggests that magnetism in $SrCo_2As_2$ is dominated by the e_g orbitals [Figs. 1(d), 1(e), 4(e), 4(f)]. These results are beyond the prevailing orbital selective Mott picture in iron pnictides, where the t_{2g} orbitals are most strongly correlated [29,33,37–39] and electron (Co) doping monotonically reduces correlations in all five d orbitals [30,31]. In addition, the FM spin correlations in $SrCo_2As_2$ are similar to the A-type AF order in $CaCo_{1.86}As_2$ [40]. Therefore, our observation is consistent with the proposal that FM fluctuations are detrimental to superconductivity in Co-overdoped $AFe_{2-x}Co_xAs_2$ and may be responsible for the hole-electron asymmetry of the superconducting dome in iron pnictide families [16].

We begin by showing constant-energy slices of $\chi''(\mathbf{Q}, E)$ on $SrCo_2As_2$ at $T = 5$ K [Figs. 2(a), 2(c), 2(e), 2(g)] [23,38]. At $E = 8$ meV, the AF spin fluctuations at $\mathbf{Q}_{AF} = (1, 0)$ are longitudinally elongated similar to that in hole-doped $BaFe_2As_2$ [Fig. 2(a)] [17]. With increasing energy, spin fluctuations along the longitudinal direction are further elongated while they barely change along the transverse direction, different from the transversely elongated spin fluctuations in $AFe_{2-x}Co_xAs_2$ [6,17]. At $E \geq 50$ meV, there are magnetic intensities at both the $\mathbf{Q}_{AF} = (1, 0)$ and $\mathbf{Q}_{FM} = (2, 0)$. Spin fluctuations form ridges of scattering across the whole Brillouin zone forming a square network [Figs. 2(e), 2(g)], similar to those in $CaCo_{2-y}As_2$ [20]. Along the transverse direction, we observed a linearly broadening of the half-width at half-maximum (HWHM) of AF spin fluctuations with increasing energy at the speed of $\Delta\text{HWHM}/\Delta E \approx 1/(440 \text{ meV Å})$ [23] and no peak splitting was identified.

We used DFT + DMFT calculations to understand the electronic band structure [Fig. 1(d)] and spin dynamics of $SrCo_2As_2$ [23,30,41]. Figures 2(b), 2(d), 2(f), and 2(h) show the DFT + DMFT calculated results for $E = 10$, 20, 50, 70 meV. Although the calculated results look remarkably similar to experimental data in Figs. 2(a), 2(c), 2(e), and 2(g), there are also important differences. First, the AF spin fluctuations are weaker than the FM spin fluctuations in the DFT+DMFT calculation at $E = 10$ meV, while they are stronger in experiments. This is mostly because the calculations are exceedingly sensitive to the position of the flatband with respect to the Fermi level. Second, the calculation suggests that FM spin fluctuations originating from the Γ (and equivalent) point merge into AF spin fluctuations at $\mathbf{Q}_{AF} = (\pm 1, 0)/(0, \pm 1)$ around 50 meV [Fig. 2(f)], while there is no clear evidence of FM spin fluctuations at $E = 8$,

19 meV [Figs. 2(a), 2(c)] [23]. Figure 1(g) shows energy dependence of local dynamic susceptibility $\chi''(E)$, obtained by integrating both the FM and AF signal within the area of $(0, 0) \to (1, 1) \to (2, 0) \to (1, -1) \to (0, 0)$ [6], and its comparison with those of $BaFe_2As_2$ [28]. The total fluctuating moment is approximately $\langle m^2 \rangle \approx 0.4 \pm 0.1$ $\mu_B^2/\text{f.u.}$ [23,28], compared with 0.5 $\mu_B^2/\text{f.u.}$ from the calculation. Because of the diffusive nature of the magnetic scattering (Signal or SIG), it is rather difficult to experimentally separate the integrated FM and AF signal and compare with that of the DFT + DMFT calculations.

To conclusively determine the FM signal in $SrCo_2As_2$, we carried out polarized neutron scattering experiments with the neutron polarization directions x, y, and z shown in Fig. 3(a), which correspond to neutron spin-flip (SF) scattering cross sections σ_x^{SF}, σ_y^{SF}, and σ_z^{SF}, respectively [42–47]. The magnetic scattering of $SrCo_2As_2$ should then be $\text{SIG} = \sigma_x^{SF} - (\sigma_y^{SF} + \sigma_z^{SF})/2$ [43–47]. Figures 3(c) and 3(d) show the energy scans at $\mathbf{Q}_1 = (1, 0, 1)$ and $\mathbf{Q}_2 = (0, 0, 3)$ [Fig. 3(a)]. Figure 3(e) shows energy dependence of SIG at $\mathbf{Q}_1$ and $\mathbf{Q}_2$, confirming the presence of magnetic fluctuations at the AF and FM wave vectors, respectively.

At $\mathbf{Q}_1$ [Fig. 3(c)], $\sigma_y^{SF} \approx \sigma_z^{SF}$ implies that the AF spin fluctuations are isotropic in spin space, different from the anisotropic spin fluctuations in $BaFe_{2-x}Co_xAs_2$ induced by spin-orbit coupling [43–47]. These results suggest that the spin-orbit coupling in $SrCo_2As_2$ is weaker than that of $BaFe_2As_2$. At $\mathbf{Q}_2$ [Figs. 3(d), 3(e)], magnetic scattering increases with increasing energy with no spin gap above $E = 3$ meV, providing direct evidence for the FM spin fluctuations in $SrCo_2As_2$ [15,23]. To further demonstrate the coexisting FM and AF spin fluctuations, we performed constant-energy scans along the $[H, 0, 3]$ and $[H, 0, 1]$ directions at $E = 8$ meV [Fig. 3(b)]. Figure 3(f) indicates that the FM spin fluctuations are confined near (0,0,3) and are about half the size of that of the AF signal around (1,0,1). The DFT + DMFT calculations predict the dominant FM spin fluctuations around 10 meV [Fig. 2(b)]. Constant-energy scans along the $[1, 0, L]$ [Fig. 3(g)] and $[0, 0, L]$ [Fig. 3(h)] directions reveal weakly L dependent scattering at both the AF and FM positions, respectively, confirming the quasi-two-dimensional nature of the magnetic scattering. Figure 1(h) shows energy dependence of $\chi''(\mathbf{Q}, E)$ at $\mathbf{Q}_{AF}$ and $\mathbf{Q}_{FM}$, where the peak in $\mathbf{Q}_{FM}$ near 25 meV should be associated with the Van Hove singularity of the flatband.

To understand the origin of the FM and AF spin fluctuations in $SrCo_2As_2$ [Fig. 4(a)], we measured its band structure by ARPES and compared the outcome in Fig. 4(c) with the DFT + DMFT calculations in Fig. 4(d). Around the Γ point, one shallow electronlike α band and one highly dispersive holelike β band were observed. Another electronlike band at the M point was also found. These results agree well with the DFT + DMFT calculation in Fig. 4(d), supporting the existence of a flatband along the Γ-M
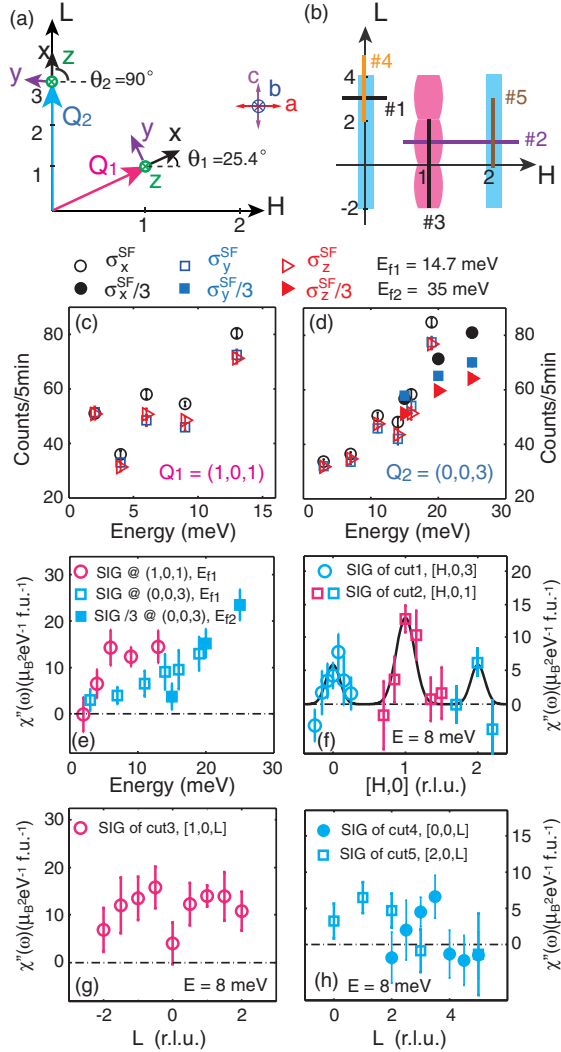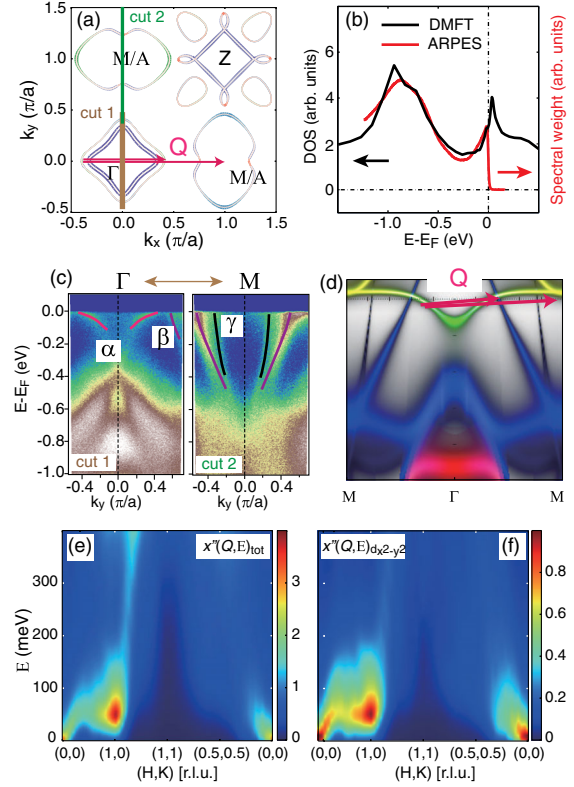
FIG. 4. (a) Fermi surfaces of $SrCo_2As_2$ from the DFT + DMFT calculations. (b) Calculated electronic DOS and integrated spectral weight from ARPES. (c) Intensity plots of the band dispersion along the Γ-M direction ($E_{photon} = 22$ eV). (d) Calculated band structure along the M-Γ-M direction. Arrows indicate possible wave vectors from occupied to empty states on the flatband. (e) Total $\chi''(\mathbf{Q}, E)$ from the DFT + DMFT calculation. (f) Calculated $\chi''(\mathbf{Q}, E)$ from the $d_{x^2-y^2}$ orbital.

FIG. 3. (a) Schematic of the $[H, 0, L]$ scattering plane for neutron polarization analysis. The AF and FM wave vectors are labeled as $\mathbf{Q}_1$ and $\mathbf{Q}_2$, respectively. The neutron polarization directions are along the x, y, and z. (b) Locations of FM (blue) and AF (magenta) spin fluctuations in reciprocal space. Lines indicate scan directions. (c),(d) Constant-$\mathbf{Q}$ scans of σ_x^{SF}, σ_y^{SF}, and σ_z^{SF} at $\mathbf{Q}_1$ and $\mathbf{Q}_2$, respectively, at $T = 1.5$ K. (e) Constant-$\mathbf{Q}$ scans of pure magnetic scattering intensity at $\mathbf{Q}_1$ and $\mathbf{Q}_2$. (f),(g),(h) The AF (magenta) and FM (blue) scattering at $E = 8$ meV along the H and L directions as marked in (b). The values of SIG are converted into absolute units by assuming the polarized data at $\mathbf{Q}_{AF} = (1, 0, 1)$ and $E = 8$ meV are comparable with the integrated intensity in $0.975 < H < 1.025$ and $-0.1 < K < 0.1$ in Fig. 2(a).

direction right above the Fermi level [Figs. 1(d) and 4(d)] [23]. Further ARPES data collected along the Z-A direction with a different photon energy reveals the presence of the flatband (or band bottom) touching the Fermi level at the A point, mainly arising from the $d_{x^2-y^2}$ orbital hybridized with the d_{z^2} [Fig. 1(d)] [23]. In particular, the partial DOS of the Co $3d_{x^2-y^2}$ orbital in the DFT + DMFT calculation exhibits

a peak at about 35 meV above the Fermi level, similar to the maximum scattering of the FM spin fluctuations [Fig. 1(h)], suggesting a close relationship between the flatband and FM instability.

Flat electronic bands with high DOS near the Fermi level can influence the electronic and magnetic properties of solids through tuning the electron-electron correlations [1–3]. In $SrCo_2As_2$, the flatband might affect spin fluctuations in two ways. First, the $d_{x^2-y^2}$ band (α) dispersive along the Γ-X/Y direction but flat along the Γ-M direction [Fig. 1(d)] might lead to high DOS near the Fermi level and Stoner FM instability similar to that of Sr_2RuO_4 [48,49]. Both the DFT + DMFT calculations and ARPES experiments reveal a prominent peak in DOS near the Fermi level [Fig. 4(b)], supporting the existence of flatband related FM fluctuations. Second, the flatband above the Fermi level provides many electron scattering channels as shown by the arrows in Fig. 4(d). These scattering processes result in the longitudinally elongated spin fluctuations extending from Γ to M [Fig. 1(f)]. This is different from the longitudinally elongated low-energy spin fluctuations in

hole-doped $BaFe_2As_2$, where the longitudinal elongation is driven by mismatched sizes of the hole-electron Fermi surfaces [17,50–52]. Figures 4(e) and 4(f) plot the DFT + DMFT calculated total dynamic spin susceptibility and contributions from the $d_{x^2-y^2}$ orbital [23]. Surprisingly, both the AF and FM spin fluctuations are dominated by the e_g orbitals (Fig. S5) [23], different from the majority t_{2g} contributions to the spin dynamics in iron pnictides [41]. In $SrFe_{2-x}Co_xAs_2$, the presence of AF spin fluctuations [12] is responsible for the superconductivity. The appearance of FM spin fluctuations in $SrCo_2As_2$ and their competition with the stripe AF spin fluctuations might be responsible the absence of superconductivity in heavily overdoped $SrFe_{2-x}Co_xAs_2$. The underlying orbital characters might also be an important factor for superconductivity in iron pnictides.

[*] yinzhiping@bnu.edu.cn
[†] lzh17@mail.sim.ac.cn
[‡] pdai@rice.edu

[1] H. Tasaki, Prog. Theor. Phys. **99**, 489 (1998).
[2] Y. Cao, V. Fatemi, A. Demir, S. Fang, S. L. Tomarken, J. Y. Luo, J. D. Sanchez-Yamagishi, K. Watanabe, T. Taniguchi, E. Kaxiras, R. C. Ashoori, and P. Jarillo- Herrero, Nature (London) **556**, 80 (2018).
[3] Y. Cao, V. Fatemi, S. Fang, K. Watanabe, T. Taniguchi, E. Kaxiras, and P. Jarillo-Herrero, Nature (London) **556**, 43 (2018).
[4] D. C. Johnston, Adv. Phys. **59**, 803 (2010).
[5] D. J. Scalapino, Rev. Mod. Phys. **84**, 1383 (2012).
[6] P. C. Dai, Rev. Mod. Phys. **87**, 855 (2015).
[7] P. J. Hirschfeld, M. M. Korshunov, and I. I. Mazin, Rep. Prog. Phys. **74**, 124508 (2011).
[8] D. J. Singh and M.-H. Du, Phys. Rev. Lett. **100**, 237003 (2008).
[9] I. I. Mazin, D. J. Singh, M. D. Johannes, and M. H. Du, Phys. Rev. Lett. **101**, 057003 (2008).
[10] A. S. Sefat, D. J. Singh, R. Jin, M. A. McGuire, B. C. Sales, and D. Mandrus, Phys. Rev. B **79**, 024512 (2009).
[11] A. Pandey, D. G. Quirinale, W. Jayasekara, A. Sapkota, M. G. Kim, R. S. Dhaka, Y. Lee, T. W. Heitmann, P. W. Stephens, V. Ogloblichev, A. Kreyssig, R. J. McQueeney, A. I. Goldman, A. Kaminski, B. N. Harmon, Y. Furukawa, and D. C. Johnston, Phys. Rev. B **88**, 014526 (2013).
[12] W. Jayasekara, Y. Lee, A. Pandey, G. S. Tucker, A. Sapkota, J. Lamsal, S. Calder, D. L. Abernathy, J. L. Niedziela, B. N. Harmon, A. Kreyssig, D. Vaknin, D. C. Johnston, A. I. Goldman, and R. J. McQueeney, Phys. Rev. Lett. **111**, 157001 (2013).
[13] N. Xu, P. Richard, A. van Roekeghem, P. Zhang, H. Miao, W. L. Zhang, T. Qian, M. Ferrero, A. S. Sefat, S. Biermann, and H. Ding, Phys. Rev. X **3**, 011006 (2013).
[14] R. S. Dhaka, Y. Lee, V. K. Anand, D. C. Johnston, B. N. Harmon, and A. Kaminski, Phys. Rev. B **87**, 214516 (2013).
[15] P. Wiecki, V. Ogloblichev, A. Pandey, D. C. Johnston, and Y. Furukawa, Phys. Rev. B **91**, 220406(R) (2015).
[16] R. Wiecki, B. Roy, D. C. Johnston, S. L. Bud'ko, P. C. Canfield, and Y. Furukawa, Phys. Rev. Lett. **115**, 137001 (2015).
[17] M. Wang, C. Zhang, X. Lu, G. Tan, H. Luo, Y. Song, M. Wang, X. Zhang, E. A. Goremychkin, T. G. Perring, T. A. Maier, Z. Yin, K. Haule, G. Kotliar, and P. C. Dai, Nat. Commun. **4**, 2874 (2013).
[18] X. Tan, G. Fabbris, D. Haskel, A. A. Yaroslavtsev, H. Cao, C. M. Thompson, K. Kovnir, A. P. Menushenkov, R. V. Chernikov, V. O. Garlea, and M. Shatruk, J. Am. Chem. Soc. **138**, 2724 (2016).
[19] A. Kreyssig, M. A. Green, Y. Lee, G. D. Samolyuk, P. Zajdel, J. W. Lynn, S. L. Bud'ko, M. S. Torikachvili, N. Ni, S. Nandi, J. B. Leão, S. J. Poulton, D. N. Argyriou, B. N. Harmon, R. J. McQueeney, P. C. Canfield, and A. I. Goldman, Phys. Rev. B **78**, 184517 (2008).
[20] A. Sapkota, B. G. Ueland, V. K. Anand, N. S. Sangeetha, D. L. Abernathy, M. B. Stone, J. L. Niedziela, D. C. Johnston, A. Kreyssig, A. I. Goldman, and R. J. McQueeney, Phys. Rev. Lett. **119**, 147201 (2017).
[21] A. Sapkota, P. Das, A. E. Böhmer, B. G. Ueland, D. L. Abernathy, S. L. Bud'ko, P. C. Canfield, A. Kreyssig, A. I. Goldman, and R. J. McQueeney, Phys. Rev. B **97**, 174519 (2018).
[22] J. Zhao, D. T. Adroja, D.-X. Yao, R. Bewley, S. Li, X. F. Wang, G. Wu, X. H. Chen, J. Hu, and P. C. Dai, Nat. Phys. **5**, 555 (2009).
[23] See Supplemental Material at http://link.aps.org/supplemental/10.1103/PhysRevLett.122.117204 for details of experimental setup and theoretical calculation, which include Refs. [4,11,23–27,30,35,36].
[24] P. Blaha, K. Schwarz, G. Madsen, D. Kvasnicka, and J. Luitz, *WIEN2K, An Augmented Plane Wave+Local Orbitals Program for Calculating Crystal Properties* (Karlheinz Schwarz, Technische Universität Wien, Austria, 2001).
[25] Z. P. Yin, K. Haule, and G. Kotliar, Nat. Phys. **7**, 294 (2011).
[26] K. Haule, Phys. Rev. B **75**, 155113 (2007).
[27] P. Werner, A. Comanac, L. de' Medici, M. Troyer, and A. J. Millis, Phys. Rev. Lett. **97**, 076405 (2006).
[28] L. W. Harriger, H. Q. Luo, M. S. Liu, C. Frost, J. P. Hu, M. R. Norman, and P. C. Dai, Phys. Rev. B **84**, 054544 (2011).

[29] M. Yi, Y. Zhang, Z.-X. Shen, and D. Lu, npj Quantum Mater. **2**, 57 (2017).
[30] Z. P. Yin, K. Haule, and G. Kotliar, Nat. Mater. **10**, 932 (2011).
[31] L. de' Medici, G. Giovannetti, and M. Capone, Phys. Rev. Lett. **112**, 177001 (2014).
[32] E. M. Nica, R. Yu, and Q. Si, npj Quantum Mater. **2**, 24 (2017).
[33] Q. Si, R. Yu, and E. Abrahams, Nat. Rev. Mater. **1**, 16017 (2016).
[34] Z.-H. Liu, A. N. Yaresko, Y. Li, D. V. Evtushinsky, P.-C. Dai, and S. V. Borisenko, Appl. Phys. Lett. **112**, 232602 (2018).
[35] G. Kotliar, S. Y. Savrasov, K. Haule, V. S. Oudovenko, O. Parcollet, and C. A. Marianetti, Rev. Mod. Phys. **78**, 865 (2006).
[36] K. Haule, C.-H. Yee, and K. Kim, Phys. Rev. B **81**, 195107 (2010).
[37] C. Zhang, L. W. Harriger, Z. Yin, W. Lv, M. Wang, G. Tan, Y. Song, D. L. Abernathy, W. Tian, T. Egami, K. Haule, G. Kotliar, and P. C. Dai, Phys. Rev. Lett. **112**, 217202 (2014).
[38] Y. Li, Z. Yin, X. Wang, D. W. Tam, D. L. Abernathy, A. Podlesnyak, C. Zhang, M. Wang, L. Xing, C. Jin, K. Haule, G. Kotliar, T. A. Maier, and P. C. Dai, Phys. Rev. Lett. **116**, 247001 (2016).
[39] Y. Song, Z. Yamani, C. Cao, Y. Li, C. Zhang, J. S. Chen, Q. Huang, H. Wu, J. Tao, Y. Zhu, W. Tian, S. Chi, H. Cao, Y.-B. Huang, M. Dantz, T. Schmitt, R. Yu, A. H. Nevidomskyy, E. Morosan, Q. Si, and P. C. Dai, Nat. Commun. **7**, 13879 (2016).
[40] D. G. Quirinale, V. K. Anand, M. G. Kim, A. Pandey, A. Huq, P. W. Stephens, T. W. Heitmann, A. Kreyssig, R. J. McQueeney, D. C. Johnston, and A. I. Goldman, Phys. Rev. B **88**, 174420 (2013).
[41] Z. P. Yin, K. Haule, and G. Kotliar, Nat. Phys. **10**, 845 (2014).
[42] R. M. Moon, T. Riste, and W. C. Koehler, Phys. Rev. **181**, 920 (1969).
[43] O. J. Lipscombe, L. W. Harriger, P. G. Freeman, M. Enderle, C. Zhang, M. Wang, T. Egami, J. Hu, T. Xiang, M. R. Norman, and P. C. Dai, Phys. Rev. B **82**, 064515 (2010).
[44] P. Steffens, C. H. Lee, N. Qureshi, K. Kihou, A. Iyo, H. Eisaki, and M. Braden, Phys. Rev. Lett. **110**, 137001 (2013).
[45] H. Q. Luo, M. Wang, C. Zhang, X. Lu, L.-P. Regnault, R. Zhang, S. Li, J. Hu, and P. C. Dai, Phys. Rev. Lett. **111**, 107006 (2013).
[46] F. Waßer, C. H. Lee, K. Kihou, P. Steffens, K. Schmalzl, N. Qureshi, and M. Braden, Sci. Rep. **7**, 10307 (2017).
[47] Y. Li, W. Wang, Y. Song, H. Man, X. Lu, F. Bourdarot, and P. C. Dai, Phys. Rev. B **96**, 020404(R) (2017).
[48] A. P. Mackenzie and Y. Maeno, Rev. Mod. Phys. **75**, 657 (2003).
[49] I. I. Mazin and D. J. Singh, Phys. Rev. Lett. **79**, 733 (1997).
[50] J. H. Zhang, R. Sknepnek, and J. Schmalian, Phys. Rev. B **82**, 134527 (2010).
[51] C. Zhang, M. Wang, H. Luo, M. Wang, M. Liu, J. Zhao, D. L. Abernathy, T. A. Maier, K. Marty, M. D. Lumsden, S. Chi, S. Chang, J. A. Rodriguez-Rivera, J. W. Lynn, T. Xiang, J. Hu, and P. C. Dai, Sci. Rep. **1**, 115 (2011).
[52] R. Zhang, W. Wang, T. A. Maier, M. Wang, M. B. Stone, S. Chi, B. Winn, and P. C. Dai, Phys. Rev. B **98**, 060502(R) (2018).